Acta Biochim Biophys Sin 2012, 44: 965–973 | © The Author 2012. Published by ABBS Editorial Office in association with Oxford University Press on behalf of the Institute of Biochemistry and Cell Biology, Shanghai Institutes for Biological Sciences, Chinese Academy of Sciences. DOI: 10.1093/abbs/gms086.
Advance Access Publication 25 October 2012

Original Article

Alteration of substrate specificities of thermophilic α/β hydrolases through domain swapping and domain interface optimization

Xiaoli Zhou[1,2], Honglei Wang[2], Yuhang Zhang[2], Le Gao[2], and Yan Feng[1,2*]

[1]State Key Laboratory of Microbial Metabolism, School of Life Sciences and Biotechnology, Shanghai Jiao Tong University, Shanghai 200240, China
[2]Key Laboratory of Molecular Enzymology and Engineering of Ministry of Education, Jilin University, Changchun 130023, China
*Correspondence address. Tel: +86-21-34207189; Fax: +86-21-34207189; E-mail: yfeng2009@sjtu.edu.cn

Protein domain swapping is an efficient way in protein functional evolution *in vivo* and also has been proved to be an effective strategy to modify the function of the multi-domain proteins *in vitro*. To explore the potentials of domain swapping for alteration of the enzyme substrate specificities and the structure–function relationship of the homologous proteins, here we constructed two chimeras from a pair of thermophilic members of the α/β hydrolase superfamily by grafting their functional domains to the conserved α/β hydrolase fold domain: a carboxylesterase from *Archaeoglobus fulgidus* (AFEST) and an acylpeptide hydrolase from *Aeropyrum pernix* K1 (apAPH) and explored their activities on hydrolyze *p*-nitrophenyl esters (*p*NP) with different acyl chain lengths. We took two approaches to reduce the crossover disruptions when creating the chimeras: chose the residue which involved in the least contacts as the splicing site and optimized the newly formed domain interfaces of the chimeras by site-directed mutations. Characterizations of AAM7 and PAR showed that these chimeras inherited the thermophilic property of both parents. In the aspect of substrate specificity, AAM7 and PAR showed highest activity towards short chain length substrate *p*NPC4 and middle chain length substrate *p*NPC8, similar to parent AFEST and apAPH, respectively. These results suggested that the substrate-binding domain is the dominant factor on enzyme substrate specificity, and the optimization of the newly formed domain interface is an important guarantee for successful domain swapping of proteins with low-sequence homology.

Keywords domain swapping; thermophilic esterase; α/β hydrolase superfamily

Received: June 28, 2012 Accepted: August 16, 2012

Introduction

Engineering the substrate specificity of critical enzymes is important in many areas, such as metabolic engineering, synthetic biology, and fuel or high-value products industries and so on [1]. Methods used for altering the substrate specificity by mutagenesis are mainly divided into two categories: directed evolution and rational design. The representative techniques of directed evolution are random mutation and DNA shuffling, which have been successfully applied in the functional modification of existing enzymes [2,3]. The directed evolution methods need screening of large libraries of enzyme variants and are time-consuming. Owing to the increasing knowledge about the three-dimensional structures of enzymes, the rational design gradually becomes the main approach to alter specificities of enzymes, such as site-directed mutation and domain recombination [4]. These rational methods play important roles in engineering novel proteins, which have the potential to be used in industry and medical science, and also in the study of structure–function relationships of the proteins [5].

Most proteins have multiple, different functional domains/subdomains, such as substrate-binding domain, catalytic domain, and coenzyme domain. Domain/subdomain recombination is an effective way to change enzyme specificity. Previous works focused on the domain exchange. For example, two phosphofructokinase chimeras were constructed by exchanging the N- and C-terminal fragment of the mammalian M- and C-type isozymes, and the results showed that the N- and C-terminal fragments were responsible for the affinity and allosteric of the enzyme, respectively [6]. In another work, a chimera was constructed by domain swapping of two isoforms of Ferredoxin-NADP+ reductase (FNR), which share 48% sequence identity. This chimera acquired a catalytic

efficiency, as an NADPH-dependent diaphorase, ~2 to 5 folds higher than those of both parents [7].

Interactions on the domain interface are important to maintain the stability of the multi-domain proteins [8]. Recombining domains of proteins with low-sequence identities often results in the destructions of the interactions among residues in domain interface. Therefore, optimization of the newly formed domain interface is necessary for recombination of functional chimeras. Some recent works on multi-domain proteins have shown that the functional change is often achieved through the insertion of protein domains and adjustment of the newly formed interface between them [9]. For example, Huang *et al*. [10] combined a low-affinity peptide-binding domain and a functionally inert second domain, and optimized the domain interface by directed evolution. These directed evolution processes dramatically enhanced both affinity and specificity for >500 folds and >2000 folds, respectively, which the single domain could not achieve.

Members of the α/β hydrolase superfamily catalyze diverse processes as proteolysis, ester hydrolysis, and epoxide hydrolysis [11]. They usually contain multiple domains or subdomains, and the active site usually locates at the interface of domains. The interactions between domains affect the catalytic functions by regulating the substrate binding and accessibility of catalytic residues. In this work, we exchanged the domains of two members of α/β hydrolase superfamily: a carboxylesterase from *Archaeoglobus fulgidus* (AFEST) and an acylpeptide hydrolase from *Aeropyrum pernix* K1 (apAPH). AFEST hydrolyzes *p*-nitrophenyl esters (*p*NP) with short acyl chain lengths and shows the highest activity toward *p*NPC4 (para-nitrophenyl-butyrate) [12]; apAPH is a typical member of the prolyl oligopeptidase family and shows a promiscuous esterase activity with a preference for middle chain length substrates, whose favorable ester substrate is *p*NPC8 (para-nitrophenyl-caprylate) [13]. The chimera composed of propeller domain of apAPH and catalytic domain of AFEST with an R526 insertion was named PAR, and the opposite one with seven sites mutagenesis for refinement of the newly formed domain interface was named as AAM7. Characterization of the chimeras showed that both of them inherited the high thermophilic property of the parents, but their substrate specificities were similar to the parent which provided the substrate-binding domain.

Materials and Methods

Homology modeling and estimation of the chimeric models

The coordinates of three-dimensional structures of apAPH (PDB ID: 1VE6) and AFEST (PDB ID: 1JJI) were obtained from the protein data bank. Multiple sequence alignment (MSA) of the templates and target chimeric sequences were produced by ClustalW [14], and manually refined, taking into account the structural superimposition of the templates. Structures were superimposed using PyMOL software [15], and used as templates to construct predictive models of chimeras. The chimeric structure models were constructed using the homologous modeling software program Modeller9v7 [16], and scored by PROCHECK program [17]. The models with the lowest energy were selected.

Construction, overexpression and purification of chimeras in *Escherichia coli*

The chimeras PAR and AAM7 were constructed by overlap extension polymerase chain reaction (PCR) technique [18]. The genes *ape1547* and *afest* were used as the templates. The propeller domain (*pp*) of *ape1547* was amplified using primers up (5′-CAGCAGCATATGGTGCGCATTATAATGC-3′) and down (5′- CGTCCTGTCCTCCCCGGCTATGGAGCG-3′). The catalytic domain (*cd1*) from *ape1547* was amplified using primers up (5′- GGGTTGAAAGAGTTAGGCTGGTTTGGGT -3′) and down (5′- CGAGCCGGATCCCTATCTCCTCTCCCTC′); the cap domain from *afest* was amplified by primers up (5′- ATGTAACATATGATGCTTGATATGCCA-3′) and down (5′- ACCCAAACCAGCCTAACACTTTCAACCCA-3′); the catalytic domain of *afest* (*cd2*) was amplified by primers up (5′-TCCATAGCCGGGGAGGACAGGACGATTAAG-3′) and down (5′- CGAGCCGGATCCCTAGTCGAACACAAGAAG -3′), (*Bam*HI and *Nde*I site are underlined). Then the *cd1* and *cap* were used as templates to amplify the full gene of *AAM7* and the *cd2* and *pp* were used as templates to amplify the full gene of *PAR*. The seven mutations of *AAM7* were introduced using the modified QuickChange® site-directed mutagenesis protocol [19]. The primers are as follows: L133Q/L136Q up (5′- GGAGGCAAAAGATCCAGGGCG -3′) and down (5′- GTCGCCCTGGATCTTTTGCCTCCA -3′); L264Q up (5′- GAGCTGCAGGCGCGG -3′) and down (5′-CCGCGCCTGCAGCTC-3′); M285T up (5′-ATAAACACAACGGAGGACG-3′) and down (5′- GTCCTCCGTTGTGTTTAT -3′); L293R/F297Q up (5′-GATACTCCTGCCCGCCGTCTTCTTCCTA-3′) and down (5′-TAGGAACTCGACGGCGGGCAGGAGTATC-3′) R250V up (5′-CCTCAGAACGACAGCGTTACACCGCTGAAACCC-3′) and down (5′-GGGTTTCAGCGGTGTAACGCTGTCGTTCTGAGG-3′). The primers for R526 insertion of *PAR* are: up (5′-GAATACGACAGACCGCTGAGAGAT-3′) and down (5′-ATCTCTCAGCGGTCTGTCGTATTC-3′). The PCR fragments of the complete genes were digested with *Nde*I and *Bam*HI and inserted into the pET-28a vector (Novagen, Madison, USA). After transformed into *E. coli* XL1-blue, the cloned gene was completely sequenced by Bio-Basic (Shanghai, China). The proteins were expressed in *E. coli* BL21-CodonPlus

(DE3)-RIL, and soluble protein was purified by nickel-chelating chromatography (Qiagen, Valencia, USA).

Native polyacrylamide gel electrophoresis and activity staining

Native polyacrylamide gel electrophoresis (PAGE) was performed at basic pH (separating gel, pH 8.8) with 8% polyacrylamide slab gels. Nondenaturing gels were stained by coomassie brilliant blue. For activity staining, gels were incubated in a solution (100 ml) of 100 mM Tris–HCl, pH 7.5, containing 5 mg of β-naphtylacetate (predissolved in 0.5 ml of methanol) and 25 mg of Fast Blue RR at room temperature. Reactions were stopped after 15–30 min by rinsing with tap water and placing gels in 7.5% (v/v) acetic acid.

Measurement of steady-state kinetics

Esterase activities were determined using *p*NP with different chain length as substrates, respectively. The amount of *p*-nitroaniline released from *p*-nitrophenyl was monitored at 405 nm using a UV-2550 spectrophotometer (Shimadzu, Kyoto, Japan). One unit of esterase activity was defined as the amount of protein that released 1 μmol *p*-nitrophenol per minute. The standard assay was performed in 20 mM wide range buffer (containing 20 mM acetic acid, 20 mM MES, 20 mM HEPES, 20 mM TAPS and 20 mM CAPS, and the pH was adjusted to the optimum pH at corresponding temperature with 1 M NaOH) at 80°C. The assay for AFEST was performed in 40 mM Na_2HPO4/NaH_2PO_4 buffer pH 8.0 containing 1% (v/v) Tween-20. The kinetic parameters K_m and k_{cat} of the parents and the chimera AAM7 were determined using *p*NP-substrates. The initial steady-state velocities of substrate hydrolysis were monitored at 9–12 different substrate concentrations. All measurements were made in duplicate or triplicate. The kinetic parameters were determined from the rates of hydrolysis by fitting the initial velocities to the Michaelis–Menten equation $[v_0 = k_{cat}[E]_0[S]_0/([S]_0+K_m)]$. All kinetic data were analyzed by nonlinear regression using MicroCal Origin software (OriginPro 8.0).

Measurement of the pH-rate profile

The pH dependence of the esterase activities were determined using 20 mM wide range buffer pH 5–10.5 using *p*NPC8 as substrate. The reaction temperature was generally 80°C.

Thermophilicity and thermostability

The optimal temperature for the hydrolysis of *p*NPC8 was determined by measuring the rate of the reaction at temperatures ranging from 40°C to 95°C. Activities were determined in wide range buffer at pH 8.0, and 2.0 mg/ml protein. For studying the thermostability, the purified enzymes (1 mg/ml, in 20 mM wide range buffer, optimum pH) were incubated in sealed tubes at 70°C. Samples were withdrawn at various times and assayed at 80°C by the standard assay. The average thermal inactivation rate constants (k_{inact}) were calculated from the plots of ln(v) versus time. The half-lives were calculated by equation $t_{1/2} = \ln 2/k_{inact}$.

Far-UV circular dichroism spectra of enzymes

Measurements were carried out using a Jasco J-815 circular dichroism (CD) spectropolarimeter and 5 mM wide range buffer at the pH optimum for each enzyme, with a protein concentration of 0.1 mg/ml, at room temperature. The path length was 0.1 cm; scan range of wavelength was from 260 nm to190 nm. The analysis of the CD spectra was performed using the CDPro software package [20].

Results

Design of the chimeras AA and PA

The sequence identity of AFEST and apAPH is only 15%, but the catalytic domains of them are very similar, with rmsd 2.6Å. The substrate-binding domains of AFEST and apAPH are very different, a 50 residues cap domain constituted of three α helices of AFEST and a seven blades β propeller domain of apAPH, respectively. We set to construct chimeric enzymes by exchanging the propeller domain of apAPH with the cap domain of AFEST.

We analyzed the number of contacts the residues in domain boundaries of the two enzymes involved in by using the LPC/CSU server (http://ligin.weizmann.ac.il/lpccsu/) [21]. The results showed that the residues involved in the minimum contacts are the Gly 332 of apAPH and Val 56 of AFEST (**Supplementary Fig. S1**). To minimize disruption of the domain interface interactions, we chose these two residues as splicing sites to construct the chimeras. We named the chimera constructed of cap domain of AFEST and catalytic domain of apAPH as AA, and the opposite one as PA. The model structures of the chimeras were constructed using the program Modeller9v7, joining the cap domain of AFEST (amino acids 1–56) with the catalytic domain of apAPH (amino acids 333–581) and the propeller domain of apAPH (amino acids 1–332) with the catalytic domain of AFEST (amino acids 57–311). After evaluating the quality of the models by Procheck and profile_3D program, we chose the best conformation for subsequent experiments (**Fig. 1**).

Analyzing and optimization of domain interfaces of chimeras

The genes of chimeras AA and PA were constructed by overlap extension PCR technique using genes of *apAPH* and *AFEST* as the templates, and expressed in *E. coli*

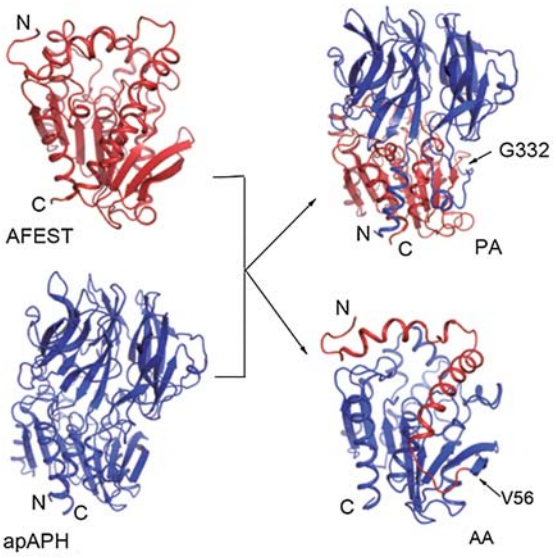

Figure 1 The structures of parents AFEST (red, PDB ID: 1JJI) and apAPH (blue, PDB ID: 1VE6), and the model structures of chimera PA, AA The crossover points are indicated. The coordinates of parents' structures were obtained from the protein data bank. The model structures of chimera PA and AA are constructed by homology modeling software Modeller 9v7.

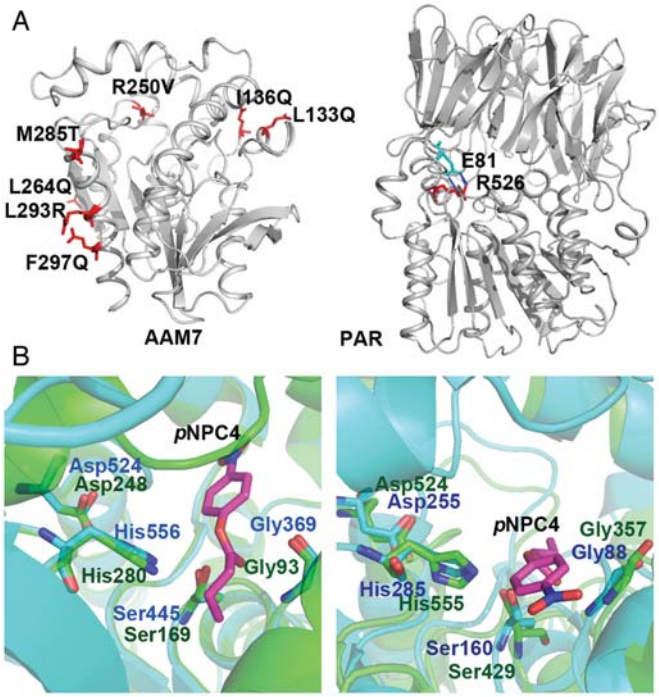

Figure 2 The model structures of the chimeras (**A**) The mutated residues of AAM7 (left) and PAR (right). The residues mutated are shown as red sticks and the residue numbers are labeled. The blue dash lines shown the polar contacts formed by R526 and E81 of PAR. (**B**) The superimposition of catalytic sites of AAM7 with apAPH (left) and PAR with AFEST (right). The *p*NPC4 substrates are shown in magenta; the chimeras AAM7 and PAR are shown in green, the parent apAPH and AFEST are shown in cyan; the catalytic triads and the oxyanion hole Gly are shown in sticks and the residue numbers are indicated.

(**Supplementary Fig. S2**). Unfortunately, we only obtained the soluble chimera PA, whereas the AA was mainly existed in the precipitation components. We compared the model structures of chimeras with the parental structures to find the reason for this phenomenon. We analyzed the interactions formed by the residues on the domain interfaces of parent apAPH, AFEST, and chimeras AA, PA, respectively, by using Ligplot software [22]. Comparison of AA and apAPH showed that on domain interface of apAPH, there are many residues involved in hydrophobic interactions and buried inside the structure [**Supplementary Fig. S3(A)**]. However, after the construction of chimera AA, some of the buried residues are exposed, such as L133, I136, L264, M285, L293, and F297 (equivalent to L409, I412, L540, M561, L569, and F573 of apAPH) [**Fig. 2(A)** and **Supplementary Fig. S3(B)**]. The exposure of these hydrophobic residues might cause the chimera misfolding and inactivation. So we mutated these residues into hydrophilic residues based on the according residues of parent AFEST, such as L133Q, I136Q, L264Q, M285T, L293R, and F297Q, respectively. Besides, in our previous studies, we found that the mutant R526V enhanced esterase activity of apAPH remarkably [23]. In order to obtain the chimera with high esterase activity, we introduced this site-mutagenesis on the chimera, the R250V. We term this seven-site mutant as AAM7. The model structure of AAM7 was constructed *in silico*.

The results of chimera PA showed that there were a large number of hydrophobic and hydrogen bonding interactions between the propeller domain from apAPH and the catalytic domain from AFEST [**Supplementary Fig. S3(C)**]. Hydrophobic interaction between the domains is an important factor for the enzyme maintaining the correct conformation and catalytic activity. It is noteworthy that, between residues on catalytic domain and residues E1, F2, I5, L12, I13, V9, E10, K17, there existed hydrophobic interaction and also formed many hydrogen bonds. Previous work in our lab reported the important role of the N-terminus 21 residues helix of apAPH [23]. Residues of this helix formed a number of hydrophobic and polar interactions with the residues on adjacent part of the catalytic domain to stabilize the protein structure. These results suggested that PA maintained the similar domain interface interactions with the parent apAPH, indicating that the PA can be correctly folded, and functionally expression. In our previous work, we have found the critical role of the inter-domain salt bridge formed by Arg526 and Glu88 of apAPH for protein stability [24,25]. Therefore, we introduced the Arg526 into the chimera PA to increase its stability. We superimposed and compared the model structure of PA with the structure of apAPH, and selected the 526 site of PA to insert the

Arg. After homology modeling, we selected the model structure with minimized energy and named it as PAR [**Fig. 2(A)**].

The Procheck analysis of the energy minimized model of PAR and AAM7 showed that almost all the residues were found in allowed regions of the Ramachandran plot. Moreover, among the total amino acids, over 92% of residues were positioned in the most favorable regions of the Ramachandran plot (**Supplementary Fig. S4**). The *p*NPC4 substrate was docked into the binding site of PAR and AAM7 by using the CDOCK module of Accelrys Discovery Studio software. **Figure 2(B)** shows the catalytic triads residues (Ser169, His280, and Asp248 in AAM7; Ser429, His555, and Asp524 in PAR) of the chimeras that are consistent with the parents (Ser445, His556, and Asp524 in apAPH; Ser160, His285, and Asp255 in AFEST). As the inter-domain interactions significantly contribute to the protein structure stability, we also calculated the domain interaction energy of the chimeras to examine the domain interface stabilities of the chimeras (**Supplementary Table S1**). The results calculated by the Accelrys Discovery Studio software showed that the recombined domains of the chimeras could form strong van der waal's and electrostatic interactions as parents.

Construction, expression, and purification of the chimeras PAR and AAM7 *in vitro*

The mutant PAR and AAM7 were constructed by Quickchange PCR and expressed in *E. coli* as soluble enzyme (**Supplementary Fig. S2**). The native PAGE electrophoretic characterization of the chimeras showed that the apparent molecular masses of PAR and AAM7 in nondenaturing conditions are about 180,000 and 70,000 daltons (**Fig. 3**). This result suggested that they were in the active trimer and dimer form, respectively. A comparison of the far-UV CD spectra of chimeras and their parent enzymes indicated that PAR and AAM7 retained the parental folds (**Fig. 4**).

Effect of temperature on the activities of the parent and chimeras

Activities for the parents AFEST, apAPH and chimeras PAR, AAM7 were determined with the substrate *p*NPC8 over a wide range temperature (40–90°C). Similar to apAPH, the optimal temperature of PAR was over 90°C, and its activity was undetectable under 50°C. The optimal temperature for the enzymatic activity of the AAM7 was 80°C [**Fig. 5(A)**], which is similar to AFEST. The chimera maintained about 90% of the maximal activity even at 90°C. At lower temperature, AAM7 still showed activity, exhibiting about 20% of the maximal activity at 50°C. Below 60°C, the activity of AAM7 increased quickly with temperature increasing, whereas above 60°C, the activity increased slower. This trend is similar to the parent AFEST,

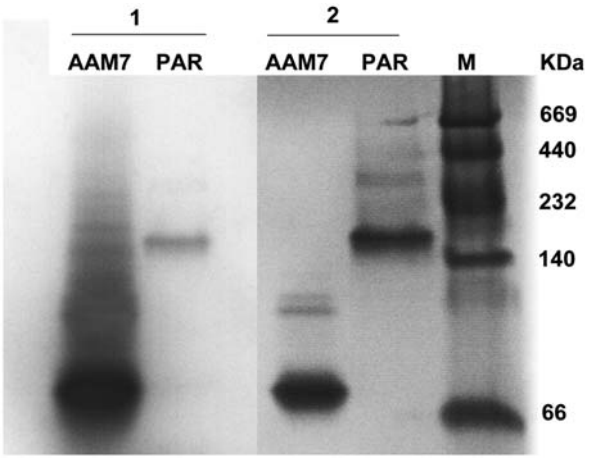

Figure 3 Native PAGE electrophoretic characterization of PAR and AAM7 1, activity staining; 2, coomassie brilliant blue staining; M, molecular weight marker.

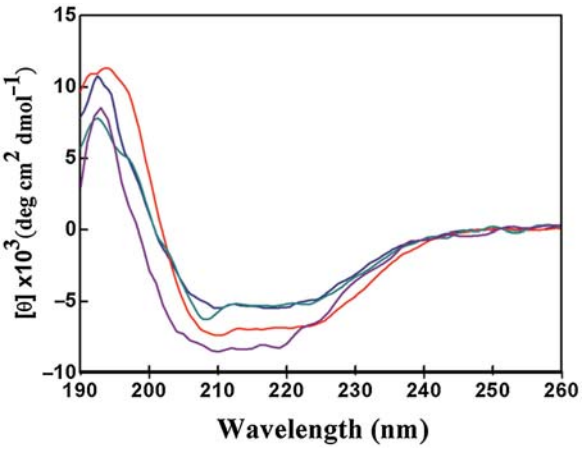

Figure 4 Far-UV CD spectra of the parents and chimeras Measurements were carried out using a protein concentration of ~0.1 mg/ml at room temperature. red, AFEST; blue, apAPH; green, AAM7; purple, PAR.

which has an inflection point at 70°C. This result implies that the rigidity of the whole molecule reduced due to the substitution of the propeller domain with the cap domain, and benefited the catalysis at low temperatures.

pH dependence of the activities of the parent and chimeras

In order to investigate the influence of domain recombination on the active-site microenvironment of the chimeras, we compared the pH dependence of the hydrolytic activities of the parents and chimeras. PAR and AAM7 displayed high activity at alkaline pH, and their activities were undetectable at pH below 7.0. The optimal pH of PAR was 9.0, similar to parent apAPH, while the optimal pH of AAM7 was ~9.5, shifted to the alkaline region relative to both the parents [**Fig. 5(B)**]. The pK_a values of catalytic

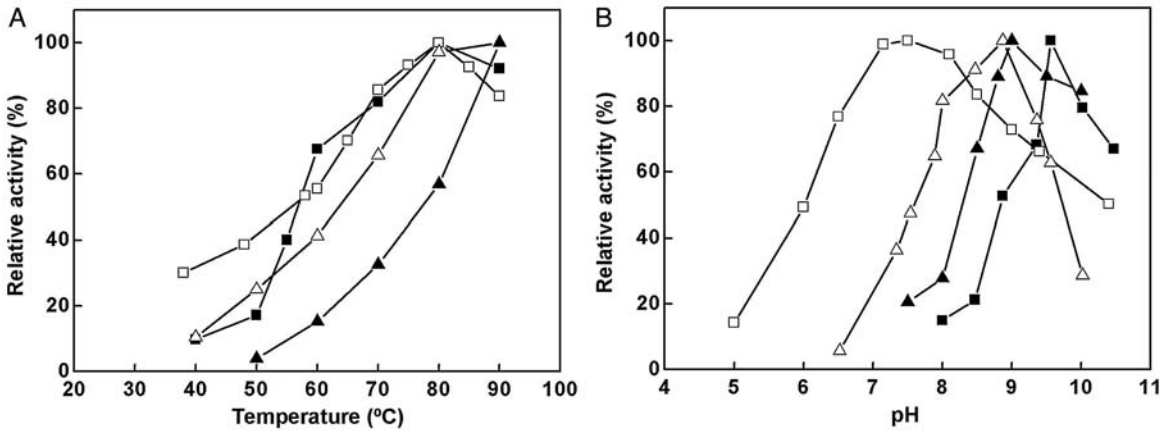

Figure 5 The effects of temperature (A) and pH (B) on the hydrolysis of *p*NPC8 by the parental enzymes, AFEST (unfilled square), apAPH (unfilled triangle) and by the chimera PAR (filled triangle), AAM7 (filled square) The temperature-dependent activities were determined with the substrate *p*NPC8 in the temperature range of 40–90°C in 20 mM wide range buffer (pH 8.0). The pH-dependent activities were determined at 80°C at a pH range of 5–10 in 20 mM wide range buffer. Data were obtained from three independent experiments.

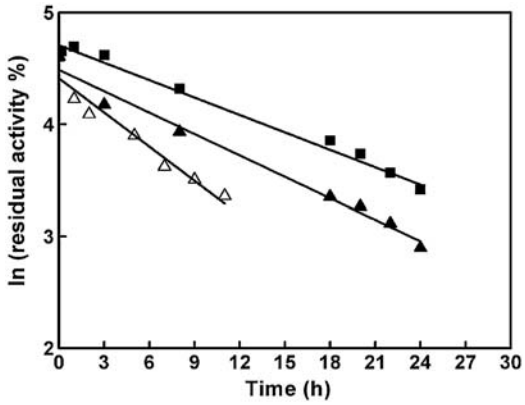

Figure 6 The thermal inactivation of chimera PA (unfilled triangle), PAR (filled triangle) and AAM7 (filled square) at 70°C The activities were determined using the *p*NPC8 as substrate. Data were obtained from three independent experiments.

histidines of AFEST, apAPH, PAR, and AAM7 calculated by PROPKA web server [26] were 6.19, 6.25, 6.35, and 6.88, respectively. We speculate that the electrostatic environment around catalytic histidines changed after domain recombination caused by subtle changes in active site and affected their deprotonation.

Thermostability of the chimeras

We measured the thermal inactivation of the chimeras at 70°C (**Fig. 6**). The results showed that the half-lives of PAR and AAM7 are about 11 and 13 h, respectively (**Table 1**), which demonstrates that these chimeras maintain the thermostability of the parents. To examine the effect of insertion of R526 on the structure stability, we also measured the thermostablity of PA at 70°C and the results are shown in **Table 1**. As expected, marked increasing of stability was observed in PAR mutant compared with PA, as the half-life of PA at 70°C was only 6.8 h. These results revealed that the R526 insertion did make an important contribution to the thermostability of the chimera.

Table 1 Parameters for thermal inactivation of chimeras at 70°C

Enzyme	k_{inact}	$t_{1/2}$ (h)
PA	0.1017	6.8
PAR	0.0637	10.9
AAM7	0.0520	13.3

Substrate specificity of chimeras

We investigated the significance of substrate-binding domains on specificity of ester substrate chain length. The kinetic parameters for parent apAPH, AFEST, and the chimeras PAR and AAM7 were initially assayed using *p*NP esters with acyl chains of various lengths at 80°C, and the results are shown in **Table 2**. Both the K_m and k_{cat} values for PAR decreased with increasing acyl chain length of the *p*NP esters. The great decrease of K_m and slight decrease of k_{cat} gave the chimeras a preference for middle chain esters, with the best substrate as *p*NPC8, consistently with apAPH. The activity of AAM7 on the long chain substrates is very low and the kinetic parameters for *p*NP-C12, C14 and C16 are undetectable. The chimera AAM7 had a clear preference for substrates with a short acyl chain, with *p*NPC4 being the best, similar to the parent AFEST. These results indicated that the cap and propeller domains are important for the substrate chain length specificities of AFEST and apAPH.

Discussion

Esterases have been widely used in industry to catalyze the stereospecific hydrolysis, transesterification, and conversion

Table 2 Kinetic parameters for hydrolysis of several pNP substrates by the parent enzymes and chimeras

*p*NP-substrates	apAPH			AFEST			PAR			AAM7		
	k_{cat} (s^{-1})	K_m (μM)	k_{cat}/K_m ($mM^{-1}s^{-1}$)	k_{cat} (s^{-1})	K_m (μM)	k_{cat}/K_m ($\mu M^{-1}s^{-1}$)	k_{cat} (s^{-1})	K_m (μM)	k_{cat}/K_m ($mM^{-1}s^{-1}$)	k_{cat} (s^{-1})	K_m (μM)	k_{cat}/K_m ($mM^{-1}s^{-1}$)
*p*NPC2	4.5 ± 0.2	178 ± 19	25.5 ± 3	120 ± 1.4	76.8 ± 3.1	1.6 ± 0.1	7.1 ± 0.1	362 ± 9	19.6 ± 0.0	0.6 ± 0.1	6.9 ± 1.1	89.3 ± 0.3
*p*NPC4	5.9 ± 0.1	115 ± 6	51.7 ± 3	277 ± 5.1	32.7 ± 2.5	8.5 ± 0.7	5.3 ± 0.3	118 ± 2	44.8 ± 0.2	8.2 ± 0.6	43.6 ± 3.4	188 ± 0.2
*p*NPC8	7.5 ± 0.3	10.7 ± 1.1	702 ± 73	831 ± 27	289 ± 23	2.9 ± 0.2	1.9 ± 0.1	30.1 ± 0.5	63.1 ± 0.2	8.7 ± 1.4	50.3 ± 8.3	172 ± 0.4
*p*NPC10	2.2 ± 0.1	3.8 ± 0.3	579 ± 91	477 ± 17	651 ± 46	0.7 ± 0.1	0.3 ± 0.0	10.5 ± 0.1	28.7 ± 0.1	2.3 ± 0.0	72 ± 2.1	32.1 ± 0.3
*p*NPC12	1.3 ± 0.1	2.9 ± 0.6	466 ± 98	128 ± 3.2	654 ± 29	0.2 ± 0.0	0.2 ± 0.0	8.0 ± 0.1	25.1 ± 0.1	–[a]	–[a]	–[a]
*p*NPC14	0.2 ± 0.0	2.6 ± 0.2	65.6 ± 6	42.3 ± 12.5	1054 ± 96	0.04 ± 0.0	0.1 ± 0.0	4.1 ± 0.1	24.6 ± 0.2	–[a]	–[a]	–[a]
*p*NPC16	0.05 ± 0.0	0.9 ± 0.1	57.3 ± 6	5.3 ± 0.4	507 ± 78	0.01 ± 0.0	0.04 ± 0.0	2.5 ± 0.1	15.9 ± 0.1	–[a]	–[a]	–[a]

[a]Undetectable.

of a variety of amines as well as primary and secondary alcohols [27]. Better understanding of the structure–function relationship of esterase, especially hyperthermophilic esterase, is meaningful for both the industry and the molecular biology. Domain recombination is an effective way to create catalyst with novel properties and to identify protein structure–function relationship. As the sequence identity of AFEST and apAPH is lower than 20%, we need to choose the appropriate recombination site to reduce the crossover disruptions when creating the chimeras. LPC/CSU is a web server for analyzing interatomic contacts in biomolecules and their complexes. Using its CSU (contacts of structural units) server, we analyzed the interactions of the residues on the domain boundaries of apAPH and AFEST involved in, and then chose the residues with the least contacts as the recombination sites. Some researchers have shown that the interdomain interactions are crucial to the conformation and consequently stability and function of enzymes [8,28]. The propeller domain of apAPH and cap domain of AFEST are very different in sequence, size, and structure. It is necessary to optimize the newly formed domain interface to minimize the destruction of the interactions between domains. Through domain swapping and domain interface optimization, chimeras PAR and AAM7 were functionally produced in *E. coli*.

Characterization of PAR and AAM7 showed that, both the chimeras retained the thermophilic of their parents, since their optimal catalytic temperature were over 80°C, with >80% of their maximal activity at 70–90°C. The pH-rate profile of AAM7 shifted to the alkaline region comparing to both parents. We speculated that there were some subtle changes in the charge environment of its active site caused by the hybrid nature of the domain interface. As the influence factors are complicated, in the future work, we will explain this phenomenon through the resolution of the crystal structure.

For esterase activity, PAR and AAM7 prefer middle- and short-chain length esters, respectively. Comparing to AFEST, the K_m values of PAR for the short-chain substrates (C2, C4) are improved about 5 folds, while for the longer chain substrates (C8–C16), the K_m values are reduced by 2–40 times. The trend of K_m values of PAR is similar to apAPH. These results suggest that the propeller domain is more suitable for the combination of long-chain substrates, while the cap domain prefer short-chain substrates. Consistent with this result, after substituted the propeller domain with the cap domain, the K_m values of AAM7 reduced 2–25 times for short-chain substrates (C2, C4) and improved 5–18 folds for longer-chain substrates (C8, C10), relative to parent apAPH. Also the trend of the k_{cat} values of PAR and AAM7 is similar to apAPH and AFEST, respectively. These results indicate that the substrate-binding domains are the dominant factor for their substrate specificities. Besides, we calculated the

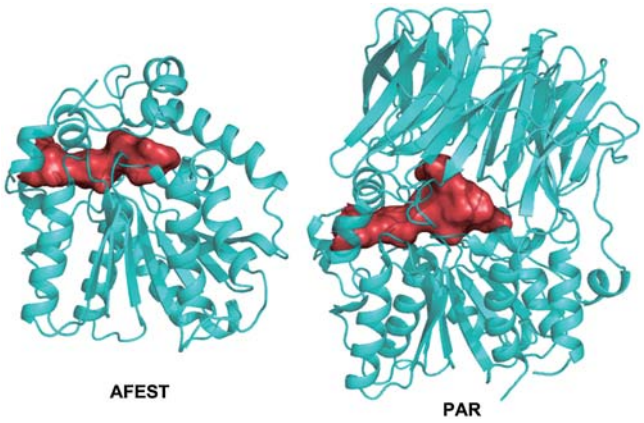

Figure 7 Substrate binding pockets of AFEST and PAR calculated by CASTp The overall structures of AFEST and PAR are shown in cyan and the pockets are shown in red surface.

substrate-binding pockets of AFEST and PAR using CASTp web server (http://sts.bioengr.uic.edu/castp) [29]. The results showed that the substrate-binding pocket became larger when the cap domain of AFEST substituted by propeller domain of apAPH (**Fig. 7**). We speculate that the larger pocket in the hybrid domain interface of the chimera PAR is suitable for the catalysis of larger substrates, and prefer the middle-chain substrate.

In summary, we constructed two active chimeric esterases through domain swapping. The characterization of chimeras indicated that the substrate-binding domains are important to the substrate specificities of α/β hydrolase family members. Our results also show that domain swapping combined with domain interface optimization is an effective way to recombine parent proteins with low-sequence identities.

Supplementary Data

Supplementary data are available at *ABBS* online.

Acknowledgement

The plasmid for the *Archaeoglobus fulgidus* carboxylesterase was a generous gift from Giuseppe Manco (Institute of Protein Biochemistry, CNR, Italy).

Funding

This work was supported by the grants from the National Basic Research Program of China (973 Program, 2012CB721000, 2011CBA00800) and the National Natural Science Foundation of China (30970632).

References

1 Pleiss J. Protein design in metabolic engineering and synthetic biology. Curr Opin Biotechnol 2011, 22: 611–617.
2 Hubner B, Haensler M and Hahn U. Modification of ribonuclease T1 specificity by random mutagenesis of the substrate binding segment. Biochemistry 1999, 38: 1371–1376.
3 Matsumura I and Ellington AD. In vitro evolution of beta-glucuronidase into a beta-galactosidase proceeds through non-specific intermediates. J Mol Biol 2001, 305: 331–339.
4 Cheriyan M, Toone EJ and Fierke CA. Improving upon nature: active site remodeling produces highly efficient aldolase activity toward hydrophobic electrophilic substrates. Biochemistry 2012, 51: 1658–1668.
5 Antikainen NM and Martin SF. Altering protein specificity: techniques and applications. Bioorg Med Chem 2005, 13: 2701–2716.
6 Martínez-Costa OH, Sánchez-Martínez C, Sánchez V and Aragón JJ. Chimeric phosphofructokinases involving exchange of the N- and C-terminal halves of mammalian isozymes: implications for ligand binding sites. FEBS Lett 2007, 581: 3033–3038.
7 Aliverti A, Pandini V and Zanetti G. Domain exchange between isoforms of ferredoxin-NADP+ reductase produces a functional enzyme. Biochim Biophys Acta 2004, 1696: 93–101.
8 Bhaskara RM and Srinivasan N. Stability of domain structures in multi-domain proteins. Sci Rep 2011, 1: 40.
9 Koide S. Generation of new protein functions by nonhomologous combinations and rearrangements of domains and modules. Curr Opin Biotechnol 2009, 20: 398–404.
10 Huang J, Koide A, Makabe K and Koide S. Design of protein function leaps by directed domain interface evolution. Proc Natl Acad Sci USA 2008, 105: 6578–6583.
11 Nardini M and Dijkstra BW. α/β Hydrolase fold enzymes: the family keeps growing. Curr Opin Struct Biol 1999, 9: 732–737.
12 Manco G, Giosuè E, D'Auria S, Herman P, Carrea G and Rossi M. Cloning, overexpression, and properties of a new thermophilic and thermostable esterase with sequence similarity to hormone-sensitive lipase subfamily from the archaeon *Archaeoglobus fulgidus*. Arch Biochem Biophys 2000, 373: 182–192.
13 Gao R, Feng Y, Ishikawa K, Ishida H, Ando S, Kosugi Y and Cao S. Cloning, purification and properties of a hyperthermophilic esterase from archaeon Aeropyrum pernix K1. J Mol Catal B Enzym 2003, 24: 1–8.
14 Thompson JD, Higgins DG and Gibson TJ. CLUSTAL W: improving the sensitivity of progressive multiple sequence alignment through sequence weighting, position-specific gap penalties and weight matrix choice. Nucleic Acids Res 1994, 22: 4673–4680.
15 DeLano WL. The PyMOL molecular graphics system. 2002. Version 1.5.0.4 Schrödinger, LLC. http://www.pymol.org.
16 Eswar N, Webb B, Marti-Renom MA, Madhusudhan MS, Eramian D, Shen MY and Pieper U, *et al*. Comparative protein structure modeling using MODELLER. Curr Protoc Protein Sci 2007, Chapter 2: Unit 2.9.
17 Laskowski RA, MacArthur MW, Moss DS and Thornton JM. PROCHECK: a program to check the stereochemical quality of protein structures. J App Cryst 1993, 26: 283–291.
18 Pogulis RJ, Vallejo AN and Pease LR. In vitro recombination and mutagenesis by overlap extension PCR. Methods Mol Biol 1996, 57: 167–176.
19 Zheng L, Baumann U and Reymond JL. An efficient one-step site-directed and site saturation mutagenesis protocol. Nucleic Acids Res 2004, 32: e115.
20 Sreerama N and Woody RW. Computation and analysis of protein circular dichroism spectra. Methods Enzymol 2004, 383: 318–351.
21 Sobolev V, Sorokine A, Prilusky J, Abola EE and Edelman M. Automated analysis of interatomic contacts in proteins. Bioinformatics 1999, 15: 327–332.

22 Wallace AC, Laskowski RA and Thornton JM. LIGPLOT: a program to generate schematic diagrams of protein-ligand interactions. Protein Eng 1995, 8: 127–134.
23 Zhang Z, Zheng B, Wang Y, Chen Y, Manco G and Feng Y. The conserved N-terminal helix of acylpeptide hydrolase from archaeon Aeropyrum pernix K1 is important for its hyperthermophilic activity. Biochim Biophys Acta 2008, 1784: 1176–1183.
24 Wang Q, Yang G, Liu Y and Feng Y. Discrimination of esterase and peptidase activities of acylaminoacyl peptidase from hyperthermophilic Aeropyrum pernix K1 by a single mutation. J Biol Chem 2006, 281: 18618–18625.
25 Yang G, Bai A, Gao L, Zhang Z, Zheng B and Feng Y. Glu88 in the non-catalytic domain of acylpeptide hydrolase plays dual roles: charge neutralization for enzymatic activity and formation of salt bridge for thermodynamic stability. Biochim Biophys Acta 2009, 1794: 94–102.
26 Bas DC, Rogers DM and Jensen JH. Very Fast Prediction and Rationalization of pKa Values for Protein-Ligand Complexes. Proteins 2008, 73: 765–783.
27 Bornscheuer UT. Methods to increase enantioselectivity of lipases and esterases. Curr Opin Biotechnol 2002, 13: 543–547.
28 Papaleo E, Renzetti G and Tiberti M. Mechanisms of intramolecular communication in a hyperthermophilic acylaminoacyl peptidase: a molecular dynamics investigation. PLoS One 2012, 7: e35686.
29 Dundas J, Ouyang Z, Tseng J, Binkowski A, Turpaz Y and Liang J. CASTp: computed atlas of surface topography of proteins with structural and topographical mapping of functionally annotated residues. Nucleic Acids Res 2006, 34: W116–W118.